# Mode-Selective Differential Scattering as a Probe of Polyatomic Ion Reaction Mechanisms

SCOTT L. ANDERSON

*Department of Chemistry, University of Utah, Salt Lake City, Utah 84112*

Received April 17, 1996

## I. Introduction

Over the past three decades there has been a tremendous body of both experimental and theoretical work aimed at understanding the mechanisms and dynamics of simple chemical reactions.[1−8] For atom + diatomic molecule reactions, theory and experiment are reaching the point of being able to determine dynamics in almost any desired level of detail. For chemical reactions between polyatomic molecules, substantial progress has also been made; however, the state of the art in both experiment and theory is far more primitive than for A + BC.

Because they have more degrees of freedom, polyatomic systems can behave in interesting ways unattainable in the A + BC world. For example, polyatomic reactants have a number of vibrational modes, with different symmetries, energies, and degrees of coupling to the reaction coordinate. This raises the possibility for mode- or bond-selective control of chemistry, including coherent control of reactions by femtosecond laser excitation.[9] A spectacular example of vibrational mode control is the reaction X (= H, Cl) + HOD → OH + DX vs OD + HX, where true bond-selective chemistry has been observed following mode-selective excitation of OH or OD stretching overtones,[10−12]or fundamental vibrations.[13] Note, however, that HOD is a special molecule, with normal vibrations that are quite localized in the OH or OD bonds. To evaluate the prospects for bond- or mode-selective chemistry in general, a more complete understanding of vibrational effects on polyatomic collisions will be needed. This is one thrust of our experiments.

The large number of degrees of freedom in polyatomic reactions can lead to other mechanistic differences compared to A + BC. The potential energy surface for reaction is more likely to have multiple local minima, corresponding to different products and to intermediate complexes that can form during the course of a reaction. If an intermediate complex does form, its lifetime can be long, allowing complicated rearrangement reactions. Complex-mediated and direct reaction mechanisms may occur simultaneously, with the competition between mechanisms controlled by collision energy, vibrational state, and reactant orientation.

Given the additional complexities of polyatomic reactions, determining detailed reaction mechanisms requires a rather detailed set of data. Our approach has been to study how different types of reactant nuclear motion (i.e., collision energy and different modes of vibration) combine to control reactivity and branching into different product channels. In addition, we measure the angular and recoil energy distributions of the products, providing information on energy disposal, collision time scale, and favored reaction geometries. The results presented below represent the first true doubly-differential cross section measurements made for mode-selectively excited ions. (Cross sections are a microscopic measure of reactivity, in our case measured as a function of product scattering angle and velocity.) For neutrals, Simpson et al.[14] have recently reported a spectroscopic approach that has allowed them to generate state-resolved differential cross sections for reaction of Cl with C−H stretch excited methane.

One of the main difficulties in these experiments is production of the mode-selectively excited reactant ions. The principles for the resonance-enhanced multiphoton ionization (REMPI) method we use are described in a recent review.[15] REMPI works well for molecular ions with proper spectroscopic characteristics; however, the technique is not general, and finding useful ionization schemes is time consuming. We have used REMPI[16−18] to study several reactions[19−27] of $C_2H_2^+$ and $OCS^+$. Other REMPI

Scott L. Anderson received his B. A. from Rice University in 1977, and a Ph.D. from the University of California at Berkeley in 1981. Following a postdoctoral fellowship at Stanford University, he joined the faculty of the State University of New York at Stony Brook in 1983. In 1995 the Anderson Group moved to the University of Utah, where he is currently a Professor of Chemistry. Anderson has research interests in the areas of ion−molecule reaction dynamics, metal and semimetal cluster chemistry, cluster-surface reactions, strained molecule isomerization, and fullerene reaction dynamics.

(1) Valentini, J. J. *Adv. Chem. Kinet. Dyn.* **1992**, *1*, 1.
(2) Marx, R. *Int. J. Mass Spectrom. Ion Processes* **661**, *118−119*, 1992.
(3) *State-selected and state-to-state ion-molecule reaction dyanmics, Part 1: Experiment, Part 2: Theory*; Ng, C. Y., Baer, M., Eds.; Wiley Interscience: New York, 1992.
(4) Miller, W. H. *Annu. Rev. Phys. Chem.* **1990**, *41*, 245.
(5) Khundkar, L. R.; Zewail, A. H. *Annu. Rev. Phys. Chem.* **1990**, *41*, 15.
(6) Levine, R. D.; Bernstein, R. B. *Molecular Reaction Dynamics and Chemical Reactivity*; Oxford University Press: New York, 1987.
(7) Zewail, A. H. *Faraday Discuss. Chem. Soc.* **1991**, *91*, 207−37.
(8) Neumark, D. M. *Acc. Chem. Res.* **1993**, *26*, 33−9.
(9) *Mode Selective Chemistry*; Jortner, J., Levine, R. D., Pullman, B., Eds.; Kluwer: Dordrecht, The Netherlands, 1991.
(10) Sinha, A.; Hsiao, M. C.; Crim, F. F. *J. Chem. Phys.* **1990**, *92*, 6333−5.
(11) Sinha, A.; Hsiao, M. C.; Crim, F. F. *J. Chem. Phys.* **1991**, *94*, 4928−35.
(12) Sinha, A.; Thoemke, J. D.; Crim, F. F. *J. Chem. Phys.* **1992**, *96*, 372−6.
(13) Bronikowski, M. J.; Simpson, W. R.; Girard, B.; Zare, R. N. *J. Chem. Phys.* **1991**, *95*, 8647−8.
(14) Simpson, W. R.; Rakitzis, T. Peter; Kandel, S. Alex; Orr-Ewing, A. J.; Zare, R. N. *J. Chem. Phys.* **1995**, *103*, 7313−35.
(15) Anderson, S. L. *Adv. Chem. Phys.* **1992**, *82*, 177−212.
(16) Orlando, T. M.; Anderson, S. L.; Appling, J. R.; White, M. G. *J. Chem. Phys.* **1987**, *87*, 852.
(17) Ashfold, M. N.; Tutcher, B.; Yang, B.; Jin, Z.; Anderson, S. L. *J. Chem. Phys.* **1987**, *87*, 5105.
(18) Yang, B.; Eslami, M. H.; Anderson, S. L. *J. Chem. Phys.* **1988**, *89*, 5527.
(19) Yang, B.; Chiu, Y. Hui; Anderson, S. L. *J. Chem. Phys.* **1991**, *94*, 6459−68.
(20) Orlando, T. M.; Yang, B.; Chiu, Y. Hui; Anderson, S. L. *J. Chem. Phys.* **1990**, *92*, 7356−64.
(21) Chiu, Y.; Fu, H.; Huang, J.; Anderson, S. L. *J. Chem. Phys.* **1995**, *102*, 1199−1216.
(22) Chiu, Y.; Fu, H.; Huang, H.; Anderson, S. L. *J. Chem. Phys.* **1994**, *101*, 5410−12.
(23) Chiu, Y. Hui; Yang, B.; Fu, H.; Anderson, S. L.; Schweizer, M.; Gerlich, D. *J. Chem. Phys.* **1992**, *96*, 5781−8.
(24) Yang, B.; Chiu, Y. Hui; Fu, H.; Anderson, S. L. *J. Chem. Phys.* **1991**, *95*, 3275−82.
(25) Orlando, T. M.; Yang, B.; Anderson, S. L. *J. Chem. Phys.* **1989**, *90*, 1577−87.


S0001-4842(95)00161-0 CCC: $14.00 

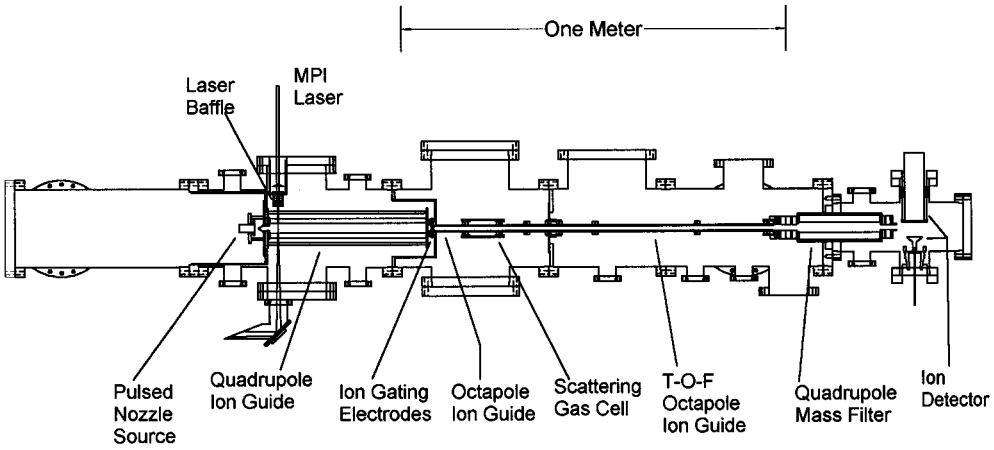


**FIGURE 1. MPI-guided ion beam instrument.**

mode-selective ion-beam work has been by Zare and co-workers,[28−30] who have studied reactions of $NH_3^+$, and also several diatomic cations.[31,32] More recently we have turned to pulsed-field ionization (PFI),[33−35] which promises to be a more general state-selection method, with broader and finer control over the ion states produced. Softley and co-workers[35,36] have recently reported the first PFI study of state-selected ion chemistry, preparing rotationally selected $H_2^+$, $N_2^+$, $NO^+$, and $CO^+$.

## II. Experimental Approach

Our ion−molecule reaction studies are carried out in the apparatus shown in Figure 1, and described in detail by Chiu et al.[21,27] Ions are produced by focusing the REMPI/PFI laser so that it intersects a pulsed beam of the neutral precursor near one end of a radio-frequency (rf) quadrupole ion guide[37] that mass and energy filters the reactant ions. Reactions are carried out by guiding the ion beam through a gas cell containing $\sim 10^{-4}$ Torr of the neutral reactant. Finally, the products and remaining reactant ions are mass-analyzed and counted.

Octapole rf fields[38] are used to guide reactant ions through the scattering cell and to collect product ions, regardless of scattering angle. The inhomogeneous rf fields in the octapole create an effective potential that confines the radial motion of the ions, while allowing free motion along the guide axis. Free axial motion allows us to use time of flight (TOF) through the ion guide to measure velocity distributions for both reactant and product ions. In some cases, we only measure a projection of the full velocity distribution on the octapole axis, but if the kinematics are favorable, it is also possible to measure the radial velocity distributions as well.[38] Analysis[27] of the $v_{axial}/v_{radial}$ distributions allows us to reconstruct the full three-dimensional recoil velocity distribution for the products, giving detailed insight into reaction mechanisms and energy disposal in the products.

## III. Example Systems

**A. $C_2H_2^+ + CH_4$.** Of the polyatomic reactions studied to date, this system shows the largest and most mode-specific vibrational effects.[21,22] A reaction coordinate diagram is given in Figure 2, showing reactants, intermediate species, and the three major low-energy product channels:

$$C_2H_2^+ + CH_4 \rightarrow C_2H_3^+ + CH_3 \qquad \Delta H = +0.02 \text{ eV} \quad (1)$$

$$\rightarrow C_3H_4^+ + H_2 \qquad \Delta H = -1.33 \text{ eV} \quad (2)$$

$$\rightarrow C_3H_5^+ + H \qquad \Delta H = -0.92 \text{ eV} \quad (3)$$

The weakly bound $C_2H_2^+\cdots CH_4$ intermediate and associated transition state (TS) are taken from recent calculations of Klippenstein,[39] and the rest of the energetics are discussed in ref 21. Note the presence of a number of covalently bound $C_3H_6^+$ species that can serve as intermediate complexes during reaction. If such a complex forms, its lifetime[40] will be in the 10 ns to 100 ps range—ample time for H-atom migration and complete energy randomization. This intermediate can decay by elimination of H, $H_2$, or $CH_3$, producing the three major products observed. Direct H-atom abstraction can also occur without a long-lived intermediate, providing a competing route to the $C_2H_3^+ + CH_3$ products.

The effects of collision energy ($E_{col}$) and reactant vibrational state on this reaction are shown in Figure 3 which gives integral cross sections ($\sigma_{reaction}$) for the three major product channels ($\sigma_{reaction}$ is a microscopic measure of total reactivity). Vibration clearly has dramatic effects, despite the fact that the accessible vibrational states have

(26) Chiu, Y.; Fu, H.; Huang, J.; Anderson, S. L. *J. Chem. Phys.* **1995**, *102*, 1188−91.
(27) Chiu, Y.; Fu, H.; Huang, J.; Anderson, S. L. *J. Chem. Phys.*, in press.
(28) Bronikowski, M. J.; Simpson, W. R.; Zare, R. N. *J. Phys. Chem.* **1993**, *97*, 2204−8.
(29) Posey, L. A; Guettler, R. D.; Kirchner, N. J.; Zare, R. N. *J. Chem. Phys.* **1994**, *101*, 3772−86.
(30) Guettler, R. D.; Jones, G. C., Jr.; Posey, L. A; Zare, R. N. *Science (Washington, D.C.)* **1994**, *266*, 259−61.
(31) Ebata, T.; Zare, R. N. *Chem. Phys. Lett.* **1986**, *130*, 467−72.
(32) Xie, J.; Zare, R. N. *J. Chem. Phys.* **1992**, *96*, 4293−302.
(33) Mueller-Dethlefs, K.; Schlag, E. W. *Annu. Rev. Phys. Chem.* **1991**, *42*, 109−36.
(34) Zhu, L.; Johnson, P. *J. Chem. Phys.* **1991**, *94*, 5769−71.
(35) Mackenzie, S. R.; Softley, T. P. *J. Chem. Phys.* **1994**, *101*, 10609−17.
(36) Mackenzie, S. R.; Halse, E. J.; Merkt, F.; Softley, T. P. In *Laser Techniques for State-Selected and State-to-State Chemistry III*; Hepburn, J. W., Ed.; SPIE-The International Society for Optical Engineering: Bellingham, WA, 1995; p 293.
(37) Schweizer, M.; Mark, S.; Gerlich, D. *Int. J. Mass Spectrom. Ion Processes* **1994**, 135, 1.
(38) Gerlich, D. *Adv. Chem. Phys.* **1992**, 82, 1−176.
(39) Klippenstein, S. J. *J. Chem. Phys.* **1996**, *104*, 5437−45.
(40) RRKM lifetime estimates corresponding to the lowest and highest collision energies studied in our experiment.

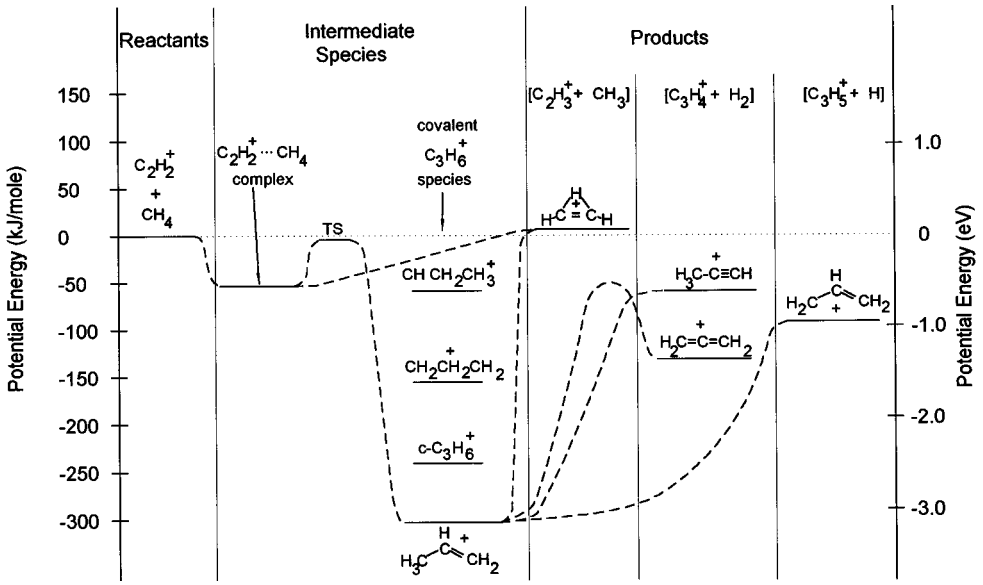


**FIGURE 2. Reaction coordinate diagram for the $C_3H_6^+$ system, showing reactants, products, and intermediates.**

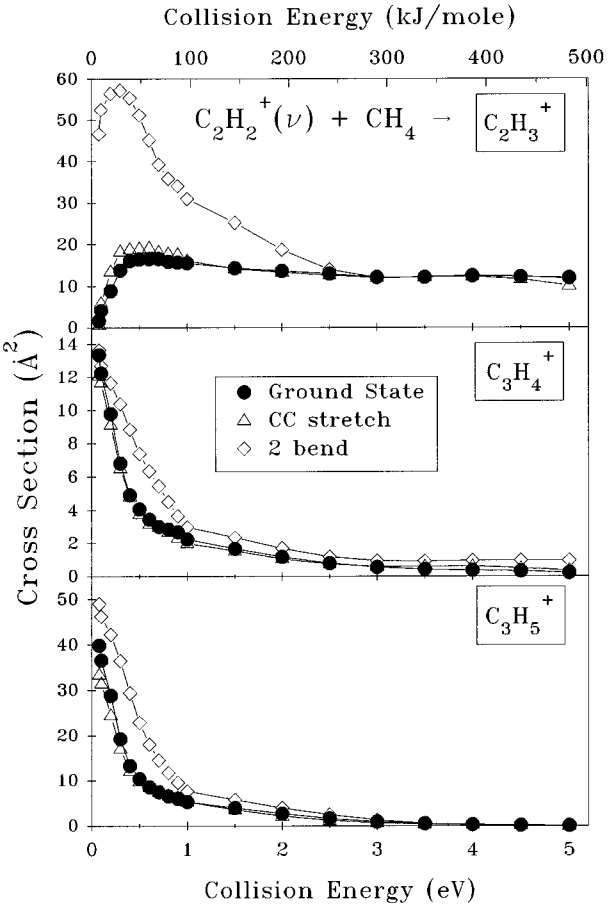


**FIGURE 3. Integral cross sections for the major products observed in low-energy reaction of $C_2H_2^+$ with $CH_4$.**

energies small compared to the $E_{col}$ range studied. The C−C stretch, $\nu_2$, has an energy of 0.225 eV (21.7 kJ/mol), while the $2\nu_{bend}$ excitation adds 0.155 eV (11.1 kJ/mol).

Both the $C_3H_4^+$ and $C_3H_5^+$ product channels are strongly inhibited by collision energy, weakly inhibited by excitation of the C−C stretch, and enhanced by bending excitation. The similar energy dependence of these two channels suggests they are controlled by a common rate-limiting step, and deuterium labeling[25] indicates that both products form via an intermediate $C_3H_6^+$ complex that lives long enough for complete H-atom scrambling. The strong dependence on vibrational mode indicates that the rate-limiting step for this reaction must be formation of the complex, because once the complex forms, energy randomization will rapidly destroy all memory of the initial mode of reactant excitation. This implies that $E_{col}$ and $C_2H_2^+$ CC stretch excitation both inhibit complex formation—not surprising since additional energy makes it more difficult for the reactant to get trapped in the $C_3H_6^+$ potential wells. In contrast, bending excitation increases the complex formation probability, despite the additional energy that must be accommodated.

The $C_2H_3^+ + CH_3$ channel has even stronger dependence on reactant energy. This reaction is slightly endoergic, and $E_{col}$ is quite effective at promoting $C_2H_3^+$ production at energies just above threshold. The $C_2H_2^+$ bending vibration has a much larger effect, enhancing the reaction by a factor of ~30 near threshold—6 times the effect of a comparable increase in collision energy. The bending enhancement also persists out to $E_{col} \approx 2$ eV—well past the point where collision energy itself becomes ineffective. In contrast, C−C stretch excitation has relatively little effect, even though this vibration provides 50% more energy than the bend. Isotope labeling experiments suggest that only ~10% of the $C_2H_3^+$ forms via $CH_3$ elimination from a $C_3H_6^+$ complex. The remaining 90% comes from a direct H-abstraction mechanism, which clearly must be powerfully enhanced by $C_2H_2^+$ bending.

Measurement of the $C_2H_3^+$ recoil velocity distributions provides more detailed insight into the nature of this direct mechanism. At high $E_{col}$, the direct H-abstraction mechanism inferred from deuterium labeling is confirmed, with the additional insight that it is a stripping process; i.e., the $C_2H_2^+$ strips an H-atom from $CH_4$ and then continues in its initial direction. At low $E_{col}$, reaction is still direct but the slower collisions are "stickier", scattering the products over a wide angular range. From

the degree of symmetry in the velocity distributions,[21] it is possible to estimate that the collision time scale varies from ≥1.3 ps at 0.4 eV to ≤70 fs at 3 eV collision energy. The velocity distributions also tell us how reactant energy is distributed in the products: In the slow collisions at low $E_{col}$, ~70% of the available energy ends up as internal energy of the products, while in the faster collisions at high $E_{col}$ nearly 55% is retained as translational energy of the products. In contrast, when energy is put into reactant vibration, a decreased fraction of the available energy appears as recoil; roughly 60% of $E_{vib}$ is retained as internal energy of the product. Bending excitation results in broader recoil energy distributions, most likely reflecting a wider range of impact parameters that contribute to the bending enhanced reaction. (The impact parameter is a measure of collision geometry. Zero impact parameter collisions are head-on and large impact parameters correspond to grazing collisions.)

The overall mechanistic picture given by these results is as follows: At very low $E_{col}$, long-lived complex formation is efficient, leading to $C_3H_4^+$ and $C_3H_5^+$ products by $H_2$- or H-elimination. Collision energy and CC stretch excitation inhibit complex formation, while bending enhances it. As $E_{col}$ increases, the efficiency of complex-mediated reaction drops and the competing direct H-abstraction reaction dominates. H-abstraction is strongly enhanced by bending, less so by collision energy, and nearly unaffected by CC stretch excitation.

The observed mode specificity implies that events early in each collision determine whether the outcome will be $C_3H_6^+$ complex formation, direct H-atom abstraction, or no reaction. On this basis, we had predicted that an early transition state must exist, and the TS recently calculated by Klippenstein[39] appears to fill the bill. Branching between complex and direct reaction is controlled by the collision energy, vibrational mode, and probably also the approach geometry. Above ~2 eV all $E_{col}$ and vibrational effects die out, and the $C_3H_x^+$:$C_2H_3^+$ branching becomes constant at ~1:2.5. The recoil velocity measurements suggest that reaction at high $E_{col}$ is controlled by the impact parameter (and probably orientation), with $C_3H_x^+$ products forming in near head-on collisions, and $C_2H_3^+$ formed mostly by stripping in high impact parameter (grazing) collisions.

From the perspective of vibrational control of reactions, an interesting question is the origin of the large bending effect on both total reactivity and the $C_3H_x^+$:$C_2H_3^+$ branching. Either reaction mechanism involves bond formation to $C_2H_2^+$, and thus requires bending of the acetylene, and rehybridization of its bonding electrons. Bending excitation clearly provides a step in the direction of the transition state, and lowers the energy required to rehybridize the $C_2H_2^+$. The transition states for the complex and direct mechanisms are presumably different, which must account for the much larger enhancement observed for H-atom abstraction. A similar transition state argument has been posited by Zare and co-workers[29,30,41,42] to explain the effects of the umbrella bend on reactions of $NH_3^+$ with several neutral molecules.

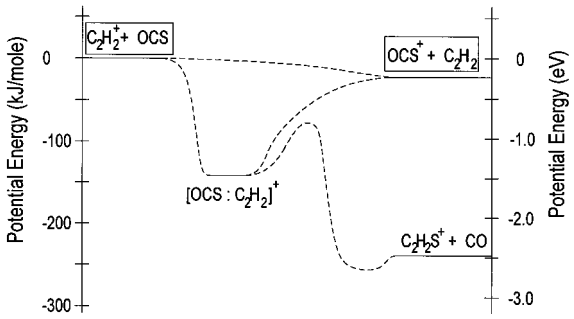


**FIGURE 4. Reaction coordinate diagram for the $[C_2H_2:OCS]^+$ system, showing reactants, products, and intermediates.**

**B. $[C_2H_2:OCS]^+$ System.** This system (Figure 4) has a pair of low-lying electronic states (charge states): the $OCS^+ + C_2H_2$ ground state and $C_2H_2^+ + OCS$ lying only 0.227 eV (22 kJ/mol) higher. We are able to state select both $OCS^+$ and $C_2H_2^+$, allowing us to probe the chemical effects of six different types of reactant nuclear motion. We recently reported[27] a detailed study of this system (including a review of the literature), and the highlights are summarized here.

The same two major reactions are observed in low-energy collisions for either reactant pair: charge transfer and $C_2H_2S^+$ production:

$$OCS^+ + C_2H_2 \rightarrow C_2H_2S^+ + CO \qquad \Delta H = -2.27 \text{ eV} \quad (4)$$

$$C_2H_2^+ + OCS \rightarrow C_2H_2S^+ + CO \qquad \Delta H = -2.51 \text{ eV} \quad (5)$$

$C_2H_2S^+$ formation is formally either S or $S^+$ transfer; in either case it is substantially exoergic. Like $C_2H_2^+ + CH_4$, this system has a potential well corresponding to an intermediate complex;[43,44] however, the complex is well above the product energy, stabilized by a barrier of unknown height. This leads to a repulsive interaction as the $C_2H_2S^+ + CO$ products separate, so that a significant fraction of the available energy is expected to go into recoil.[43]

Figure 5 shows the collision energy and vibrational state dependence of both major reactions. For the $OCS^+ + C_2H_2$ charge state, cross sections are plotted for the $OCS^+$ ground state, one or two quanta of $\nu_3$ (C−S stretch = 0.087 eV), two quanta of the bend ($2\nu_2$ = 0.125 eV), and one quantum of $\nu_1$ (C−O stretch = 0.253 eV). For $C_2H_2^+ +$ OCS, we plot cross sections for $C_2H_2^+$ in its ground state, with one or two quanta of the CC stretch ($\nu_2$ = 0.225 eV), and with two quanta of the bend ($2\nu_{bend}$ = 0.155 eV).

**1. $C_2H_2S^+$ Production.** The cross sections for $C_2H_2S^+$ production are similar for the two reactant charge states, dropping rapidly as $E_{col}$ is increased to ~0.8 eV and then becoming nearly energy independent at higher energies. The reaction efficiency ($\sigma_{reaction}/\sigma_{collision}$) drops from 30−40% at our lowest collision energy (0.08 eV) to roughly 10% at $E_{col}$ = 0.8 eV and then is roughly constant at higher energies. The vibrational effects also change rapidly in the $E_{col}$ range below 0.8 eV, then become essentially

(41) Conaway, W. E.; Ebata, T.; Zare, R. N. *J. Chem. Phys.* **1987**, *87*, 3453−60.
(42) Morrison, R. J.; Conaway, W. E.; Zare, R. N. *Chem. Phys. Lett.* **1985**, *113*, 435−40.
(43) Graul, S. T.; Bowers, M. T. *J. Phys. Chem.* **1991**, *95*, 8328−37.
(44) Orlando, T. M.; Friedmann, A.; Maier, J. P. *J. Chem. Phys.* **1990**, *92*, 7365−72.

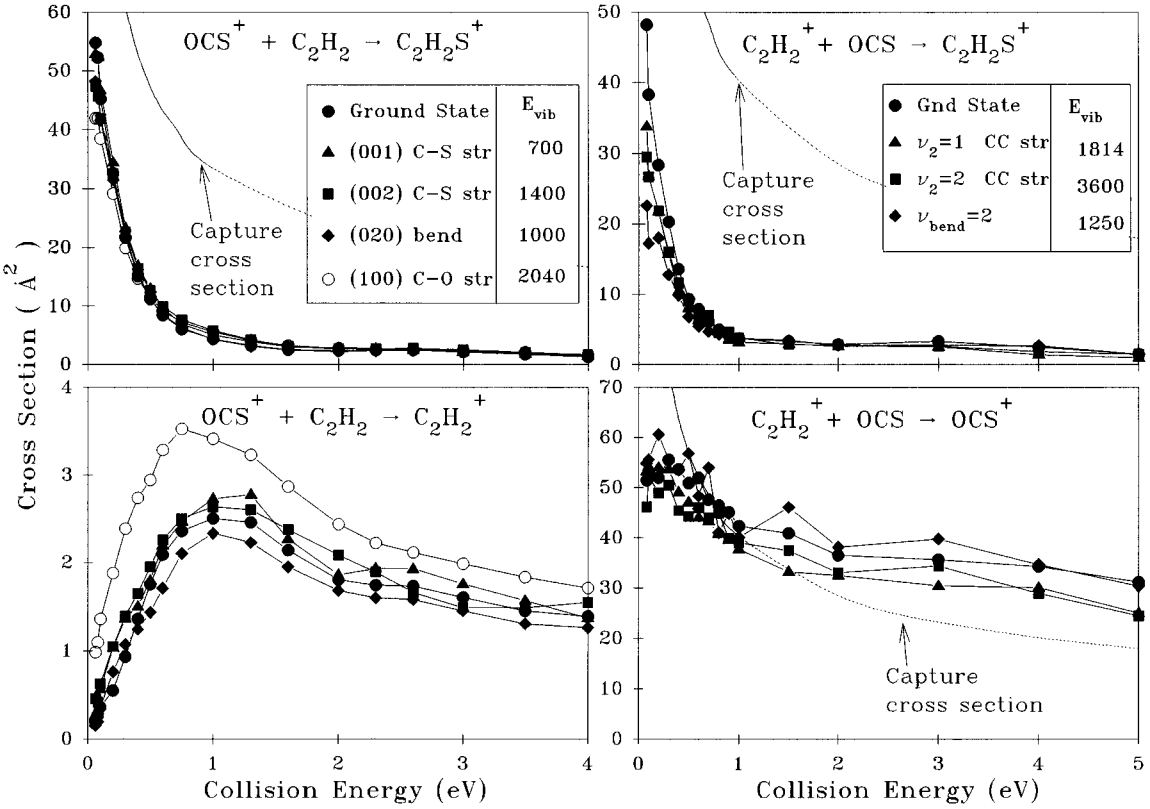


**FIGURE 5. Integral cross sections for the major products in reaction of $C_2H_2^+$ + OCS and $OCS^+$ + $C_2H_2$.**

constant. This energy dependence suggests that one reaction mechanism dominates at $E_{col} > \sim 0.8$ eV, with a different mechanism growing in as $E_{col}$ decreases toward zero. Given that $[C_2H_2{:}OCS]^+$ complexes are known to form in thermal energy collisions,[43,44] the obvious candidate for the low-energy mechanism is reaction via a long-lived intermediate complex. Since the $[C_2H_2{:}OCS]^+$ potential well is rather shallow, the strong $E_{col}$ suppression of this mechanism is not unexpected. The low, and almost energy-independent, reactivity observed at high energies suggests a mechanism controlled by collision geometry. The similarity in the $C_2H_2S^+$ cross sections for the two charge states suggests that they may react by similar mechanisms.

The recoil velocity measurements support this picture and also show the nature of the high-energy reaction mechanism. In examining the velocity maps in Figures 6 and 7, bear in mind that our resolution is rather low, ~400 m/s. While the major features are well constrained by the data, small-scale details are not, and should not be regarded as significant.

CM frame $C_2H_2S^+$ recoil velocity maps for the $OCS^+$ + $C_2H_2$ reaction are given on the left side of Figure 6 for two collision energies. At $E_{col} = 0.48$ eV (top left) the map has two main components, neither of which has the forward−backward symmetry about $v_{axial} = 0$ that would be required for a complex-mediated mechanism. Clearly these components result from a direct scattering mechanism. Note, however, that in addition to these peaks there is a diffuse component accounting for 30−50% of the product intensity. This, most likely, results from a complex-mediated reaction mechanism, which is already overshadowed by direct reaction at $E_{col} = 0.48$ (the lowest energy where we could measure recoil velocities).

There are actually two direct components. One is forward-peaked along the direction of the $OCS^+$ reactant beam, corresponding to $C_2H_2S^+$ formation by a rebound process, requiring low impact parameter (near head-on) collisions. The other prominent peak is sideways-scattered at ~110° relative to the $OCS^+$ beam, corresponding to $S^+$ transfer in glancing collisions. Increasing $E_{col}$ (bottom left, Figure 6) has little effect on the forward/rebound scattering mechanism, but the sideways component shifts progressively backward, indicating that glancing gives way to $S^+$-stripping collisions as the energy is increased.

The kinematics for the $C_2H_2^+$ + OCS charge state are poor, and we can only measure the forward-scattered half of the recoil velocity map. The results (right side of Figure 6) are consistent with the idea that the two charge states react by similar mechanisms. The rebound mechanism observed for $OCS^+$ + $C_2H_2$ should give a back-scattered peak for $C_2H_2^+$ + OCS, out of our observable range. The glancing/stripping mechanism should give a sideways-scattered peak at low energies, shifting *forward* to smaller angles with increasing $E_{col}$, as observed. We can say that the relative importance of the rebound mechanism is higher for $C_2H_2^+$ + OCS than for $OCS^+$ + $C_2H_2$, at least at high $E_{col}$. These results suggest that the two charge states are coupled (i.e., the charge "equilibrates" as the reactants come together, before chemical reaction) at low $E_{col}$, but that the coupling breaks down in fast collisions at high energies.

Vibrational effects (Figure 5) are different for the low-energy (complex-mediated) and high-energy (direct) $C_2H_2S^+$ production mechanisms. In the complex-dominated energy range, $OCS^+$ vibration causes weak, non-mode-specific inhibition, as does collision energy. This is

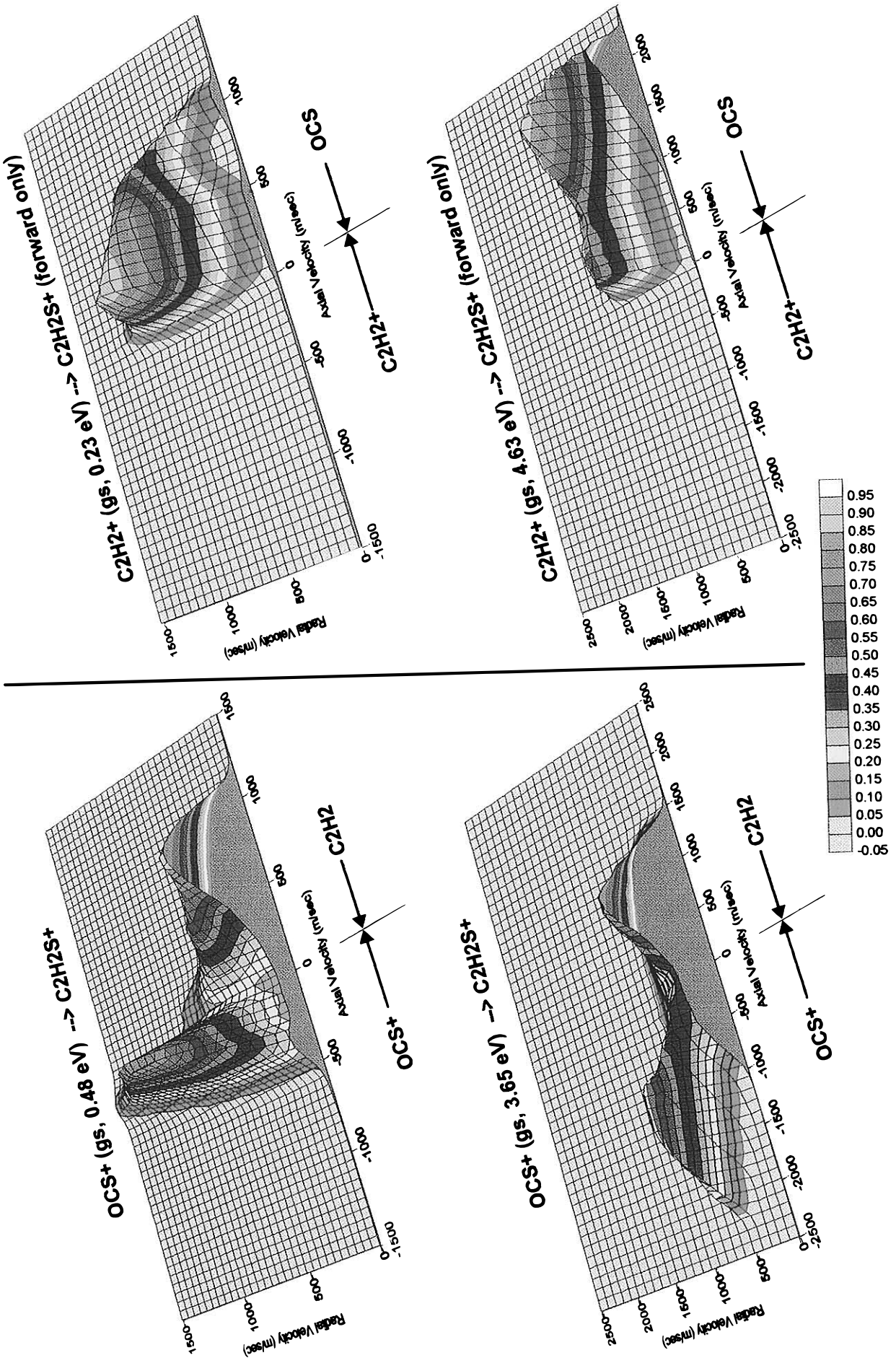


**FIGURE 6.** CM frame recoil velocity maps for the $C_2H_2S^+$ product.

expected since additional energy of any type makes it more difficult to form a long-lived complex. In contrast, $C_2H_2^+$ vibration results in larger, and more mode-specific, inhibition. In particular, excitation of the $C_2H_2^+$ $2\nu_{bend}$ vibration gives an anomalously large inhibition. This is in sharp contrast to the enormous enhancement the same vibration gives to the $C_2H_2^+ + CH_4$ reaction. We propose that the effect is controlled by the *cis*-symmetry of the bending motion. This is just the motion needed to get through the transition state for $C_2H_2^+ + CH_4$, while the transition state controlling formation of $[C_2H_2{:}OCS]^+$ is strongly *trans*-bent.[43]

In the energy range dominated by direct reaction, $C_2H_2^+$ vibration has essentially no effect, as does $OCS^+$ bending vibration and collision energy. On the other hand, both $OCS^+$ stretches enhance $C_2H_2S^+$ production, with greatest efficiency from $\nu_3$, which gives the largest motion in the OC−S bond. This is consistent with the idea that adding energy to the reaction coordinate (i.e., OC−S bond scission) should increase reactivity.

**2. Charge Transfer.** In contrast to the similarities observed for $C_2H_2S^+$ production, the charge transfer (CT) dynamics are quite different for the two reactant charge states.

CT from $OCS^+$ to $C_2H_2$ is 0.227 eV endoergic; thus, collision-to-internal energy conversion is needed to drive the electron transfer. This requires intimate collisions, and as a consequence $\sigma_{CT}$ (bottom left, Figure 5) is quite small over our entire energy range. At low collision energy, $\sigma_{CT}$ rises from a threshold, as expected for an endoergic reaction, and is strongly enhanced by both vibrational and collision energy. The velocity maps (left side of Figure 7) show that low-energy CT gives forward-scattered $C_2H_2^+$. This corresponds to rebound from small impact parameter (near head-on) collisions that evidently are required for the collision-to-internal energy conversion needed. In this threshold energy regime, all forms of vibration enhance CT, approximately in proportion to the energy, indicating that vibration is simply another source of available energy.

At higher $E_{col}$, mode-specific behavior becomes apparent (Figure 5). Collision energy and bending excitation begin to suppress charge transfer, and C−S stretch excitation has essentially no effect, but C−O stretch excitation continues to enhance, by 30−40%. These changes in $E_{col}$ and vibrational effects suggest that the reaction dynamics change with collision energy. The velocity maps (Figure 7) confirm this. As $E_{col}$ increases, the peak recoil velocity shifts sideways and then backwards, but with a substantial tail extending into the forward hemisphere. The forward-scattered products come from low impact parameter collisions that continue to be important at high energies. The back-scattering can only result from grazing collisions that account for ∼70% of CT at our highest energies. CT in grazing collisions is possible because in this energy range only a few percent of $E_{col}$ must be converted to drive CT. On the other hand, the small magnitude of the CT cross section shows that these grazing collisions are inefficient.

At $E_{col} = 0.45$ eV, CO stretch excitation ($\nu_1 = 253$ meV) nearly doubles the energy available to the products, and actually is sufficient to overcome the CT endoergicity. In other cases where vibration overcomes CT endoergicity,[45,46] order of magnitude increases in $\sigma_{CT}$ are observed, because long-range electron hopping becomes possible. Here, $\nu_1$ enhances CT by only ∼50% (Figure 5). This modest increase might seem to support some role for long-range CT; however, the velocity maps show only contributions from intimate collisions. Evidently, the coupling required to allow CO stretch de-excitation to drive long-range CT is absent. On the other hand, the vibrational energy is available to drive CT in intimate collisions, as shown by the higher recoil velocities observed for the products.

Charge transfer in the exoergic direction ($C_2H_2^+ + OCS \rightarrow OCS^+$) has a cross section (bottom right, Figure 5) more than an order of magnitude greater than that for the endoergic CT just discussed. Exoergic CT is found to be only weakly dependent on $E_{col}$ and vibrational state. At $E_{col} > \sim 1$ eV, the CT cross section ($\sigma_{CT}$) exceeds $\sigma_{collision}$, suggesting a long-range electron hopping mechanism. In this energy range the vibrational effects can be rationalized with a Franck-Condon/energy gap model,[20] providing further support for a long-range mechanism. As $E_{col}$ is lowered into the range where the capture cross section becomes large, $\sigma_{CT}$ also increases, and the vibrational effects gradually become smaller. This suggests the influence of a second reaction mechanism at $E_{col}$ below ∼1 eV—presumably capture to a more intimate collision, possibly involving a long-lived complex.

The right half of Figure 7 shows velocity maps for $OCS^+$ produced by CT from ground state $C_2H_2^+$. At low $E_{col}$ the velocity distribution is centered about zero CM velocity and significantly sideways peaked, indicating that the low-energy CT mechanism is at least partly direct. As $E_{col}$ is increased, the distribution shifts progressively into the backward hemisphere, with a tail extending forward to the limit allowed by energy conservation. The strong backward peaking is just what is expected for a long-range electron hopping mechanism; the product ion should pick up little momentum from the collision, corresponding to back-scattering in the CM frame. The forward-scattered tail shows that low impact parameter collisions also contribute to CT; however, their contribution is overwhelmed by the efficient long-range CT mechanism.

## IV. Conclusions

As these results show, measuring the effects of different forms of reactant excitation can provide detailed insight into the factors that control reaction of polyatomic species. When combined with recoil velocity measurements, quite an elaborate picture emerges of the reaction mechanisms and how they change with reactant excitation. Of the five reactions we have studied with mode-selective excitation, all have shown some mode selectivity in total reactivity and/or product branching. In some cases the vibrational effects can be rationalized in terms of transition state geometries or motion along the reaction coordinate. In

(45) Anderson, S. L.; Turner, T.; Mahan, B. H.; Lee, Y. T. *J. Chem. Phys.* **1982**, *77*, 1842−54.
(46) Houle, F. A.; Anderson, S. L.; Gerlich, D.; Turner, T.; Lee, Y. T. *J. Chem. Phys.* **1982**, *77*, 748−55.

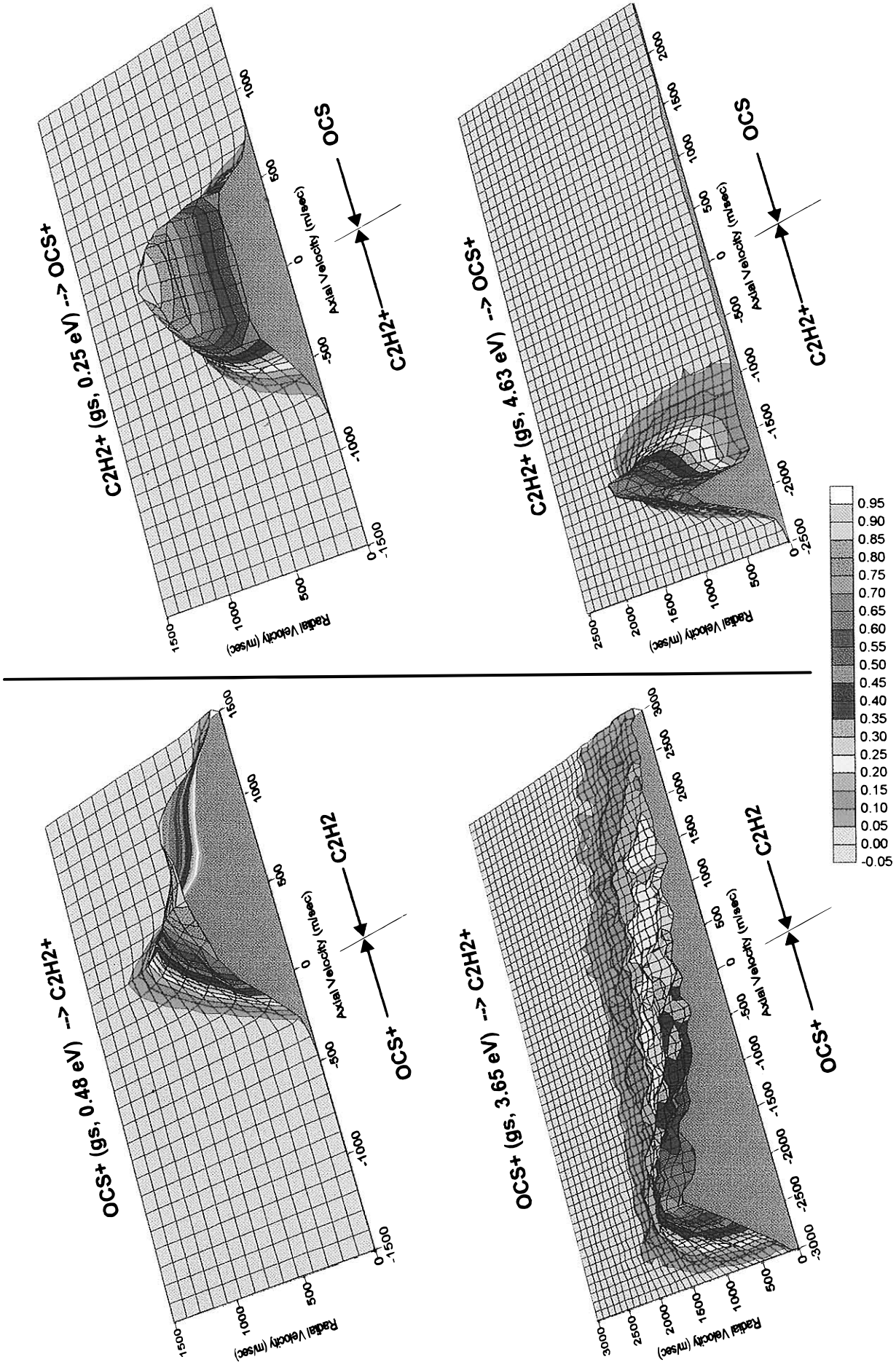


**FIGURE 7.** CM frame recoil velocity maps for the CT product.

others, the origin of the effects is not clear. Only in the $C_2H_2^+ + CH_4$ system discussed above have the effects been large enough to qualify as vibrationally-controlled chemistry. Nonetheless, the mechanistic insight gained through these studies should help refine our understanding of the types of excitation that might be required to reach that goal.

*I gratefully acknowledge continuing support from the National Science Foundation (Grant CHE 9520802). The experimental work was done by my students: Tom Orlando, Baorui Yang, Yu-hui Chiu, Jui-tsen Huang, and Hungshin Fu. Over the years I have benefited by many helpful discussions with Dieter Gerlich, the pioneer of the ion guide techniques used in this work.*

AR950161L